

TIME PROFILE OF SOLAR COSMIC RAYS – USING PITCH ANGLE DIFFUSION COEFFICIENTS DEPENDING UPON THE CHANGE OF MAGNETIC FIELD STRENGTH ALONG ARCHIMEDIAN FIELD LINES –

T. Sakai

*Department of Physics, College of Industrial Technology, Nihon University, 2-11-1 Shin-ei.
Narashino-shi, Chiba-ken, Japan*

Abstract

Propagation of energetic solar cosmic rays was studied by solving the focussed transport equation without adiabatic deceleration. In our calculations, we considered the change of pitch angle diffusion coefficient due to the variation of magnetic field strength along Archimedian interplanetary magnetic field lines in addition to magnetic field fluctuation and its correlation length depending upon radial distance from the sun. For some typical values of radial dependence of magnetic field fluctuation (e.g. power index of radial dependence = -2), we obtained the scattering mean free path at 0.1 AU 10 times longer than the one near the earth. The time profiles calculated using the above radial dependence are compared with several observations.

1 Introduction:

Solar cosmic rays in the inner heliosphere are generally assumed to propagate along large-scale interplanetary magnetic fields (Parker magnetic field line) with superimposed small-scale irregularities. The resulting adiabatic focusing and pitch angle scattering lead to the focused transport equation (Earl, 1976)

$$\frac{f}{t} + \mu V \frac{f}{z} + \frac{(1-\mu^2)V}{2L(z)} \frac{f}{\mu} - \frac{1}{\mu} (D_{\parallel}(z, \mu) \frac{f}{\mu}) = Q(z, \mu, t), \quad (1)$$

where t is time, V the particle velocity, μ the cosine of pitch angle, z the distance along the spiral magnetic field, $L(z) = -B(z)/(dB/dz)$ focusing length, $D(z, \mu)$ the pitch angle diffusion coefficient and $Q(z, \mu, t)$ the particle source close to the sun. For the convenience of our argument,

$$D_{\parallel}(z, \mu) = D_0(r, \mu, q, V) * (1-\mu^2) |\mu|^{q-1} \quad (2)$$

is adopted following quasi-linear theory, where q is the power index of the magnetic power spectrum. Hereafter, D_0 is expressed as a function of r because all observable quantities can be expressed as a function of r , where r is the distance from the sun. Then, following Jokipii (1971) and Goldstein (1976), D_0 is represented as below.

$$D_0 \sim \frac{V}{(r)} (L_c(r) / (r))^{1-q} < B(r)^2 > / < B(r)^2 >, \quad (3)$$

where (r) is the particle gyro radius, $L_c(r)$ the correlation length of magnetic fluctuation, $< B^2(r) >$ the average of square of magnetic fluctuation, and $< B(r) >$ the average of the ambient magnetic field. If we use the typical dependence of L_c and B^2 upon r , and the Parker magnetic field strength for $B(r)$, it is clear that

D_0 has a complicated radial dependence unlike the simple expression of r^{-b} , where b is a constant. This fact will reflect the radial dependence of mean free path of cosmic rays and should be emphasized as well as the importance of focusing effect, as pointed out by many authors so far, when Eq. (1) is tried to solve. We will show a solution of Eq. (1) for a typical radial dependence of B^2 and L_c .

2 Radial Dependence of Mean Free Path

The relation (e.g. Volk, 1975) between the parallel mean free path $\lambda_{\parallel}(r)$ and $D_0(r)$ is tentatively adapted here as following,

$$\lambda_{\parallel}(r) = \mathfrak{V} / (D_0(r)(2-q)(4-q))$$

Inserting D_0 into the above equation, $\lambda_{\parallel}(r)$ is then expressed as

$$\lambda_{\parallel}(r) \sim L_c^{q-1} / \langle B^2(r) \rangle / \langle B(r) \rangle^2.$$

Here, we assume $L_c \sim r^m$ and $\langle B^2(r) \rangle \sim r^{-k}$ by following Jokipii(1973). Further, we express Parker spiral magnetic field $B(r)$ as $r^{-2} \text{SQRT}(1+(r/a)^2)$, where a is the ratio of solar wind speed to the angular velocity of the sun. Altogether, we obtain

$$\lambda_{\parallel}(r) \sim r^{k+m(q-1)-2q} \{ \sqrt{1+(r/a)^2} \}^2.$$

The radial dependence of B^2 and L_c has been discussed by many authors. But here we basically follow the discussion by Jokipii(1973). That is, $k=2$ for $r \ll a$ and $k=3$ for $r \gg a$. For L_c , we adopt only the cases of $m=0$ and 0.5 .

Next, we will show several cases of radial dependence of $\lambda_{\parallel}(r)$. Shown in figure 1 are $\lambda_{\parallel}(r)$ in unit of λ_E denoting the mean free path at the earth, for the cases of $k=2$, $m=0.5$ with $q=1.5$ (upper curve in the region beyond 1 AU) and 1.67 (lower curve in the region beyond 1 AU), respectively. They indicate that λ_{\parallel} becomes larger for both $r \gg r_E$ and $r \ll r_E$. The longer λ_{\parallel} for $r \ll r_E$ is easily understood. The resonant wavelength of magnetic fluctuation becomes shorter with increasing $B(r)$ for $r \ll r_E$. Then the power density of the fluctuation tends to decrease as the wavelength shortens. Thus, the mean free path becomes longer for $r \ll r_E$. Figure 2 shows four cases of $\lambda_{\parallel}(r)$ in unit of λ_E . The uppermost curve corresponds to $k=2 \sim 3$, $m=0.5$ and $q=1.67$, the upper to $k=2 \sim 3$, $m=0$ and $q=1.67$, and the lower to $k=2$, $m=0.5$ and $q=1.67$, and also the shaded line constant to mean free path. Here, $k=2 \sim 3$ means a transition from $k=2$ to 3 at the earth in this case. Although we tentatively take the transition at the earth, we fully recognize that the transition point should be reconsidered in the future. These mean free paths are used for solving Eq. (1).

3 Time Profiles:

Fig.3 and 4 show time profiles for $\lambda_E = 0.039$ AU and $q=1.67$ at 0.5 and 1 AU respectively. The uppermost curve corresponds to $k=2 \sim 3$, $m=0.5$, the upper to $k=2 \sim 3$, $m=0$, and the lower to $k=2$, $m=0.5$, and also to the shaded line constant mean free path. The upper and lower curves in Fig.3 seem to coincide each other. From the both figures, it is clear that time profiles differ from each other according to interplanetary condition between the source and the region behind an observation point, even if the mean free path λ_E at the earth is the same. The different time profiles are due to the following facts. That is, the rising part of the intensity is mainly reflected by the size of mean free path between the source and the observation point. On the other hand, the mean free path beyond the observation point affects the decreasing phase. We examined time profiles by using various values of mean free path at the earth. We recognized that almost the same time profile with the constant mean free path can be obtained with half the length of the mean free path, if we introduce a radial dependent mean free path (e.g. $k=2 \sim 3$, $m=0.5$).

6 Discussions:

We will show an example of comparison of our results with the time profile of electrons given by Bieber et al., (1980) in figure 5. In the figure, solid squares indicate the data observed on Helios 2 on 28th March, 1976 (we read out the data from their paper), and dashed lines best-fitting prediction obtained by them with $r_E = 0.7$ AU, $\tau = 0.7$ h and $\tau = 1.5$ h from ~ 4 hours after Flare. α and β are a constant (see Reid, 1964). Also, the solid line (our case) shows the time profile obtained with $r_E = 0.039$ AU, $k=2\sim 3$, $m=0.5$ and $q=1.67$. Here, solar particles are assumed to be simply injected like $\exp(-t/90 \text{ min.})$. The injection pattern can change only the shape around the peak value. But the general tendency of the decay phase can not be changed very much by the injection. It is clear that our case can give a good fitness for the observed data of more than 10 hours. This good fitness is due to the facts that at $t < t_{\max}$, a longer mean free path than r_E is effective, and that at $t > t_{\max}$, $r_E = 0.039$ itself may be important for the propagation of solar particles. This shorter mean free path can create a longer decay phase. This means that, in some cases, we had better to take into account the radial dependence of mean free path; that is, the radial dependence of interplanetary magnetic field condition.

Further, if we compare the mean free path around the earth deduced from quasi-linear theory with the one from fitting to observed time profile, r_E which we introduced here, should be used. Otherwise, we will need all the information about magnetic fields in interplanetary space. Thus, our r_E may be directly compared with the value derived by Jokipii(1971).

5 Summary:

Generally, calculated time profile supposing the constant mean free path independent of r can be approximately reproduced by the one calculated using radial dependent mean free path, which has a shorter r_E by the factor 2. Further, in fitting to the time profile observed on 25th March 1976, more than one order of magnitude shorter mean free path ($r_E = 0.039$) can fit to the data, comparing to Bieber et al.,(1980). Of course, we have to note here that our value is converted to the one at the earth, that is r_E , although their is given at 0.5 AU. We can designate the mean free path at the earth. So r_E determined by our method seems appropriate in comparing directly with the mean free path given by Jokipii(1971), since he used power spectrum at the earth. Further, if we consider the above facts, our method may be helpful in reducing the discrepancy of one order pointed out by Palmer(1981). On the other hand, some theorists are trying to get longer mean free path, which may also reduce the discrepancy by a factor of order unity. Thus, considering altogether, that is, including our method and also improvement of theory, the one order difference may be reconciled in the near future.

6 References:

- Droge, W., et.al., 1997, Proc. 25th ICRC(Durban), **1**, 137.
- Earl, J.A., 1976, ApJ., **205**, 900.
- Goldstein, M.L., 1977, JGR. , **82**, 1071.
- Hatzky, R. and Wibberenz, G, 1997, Proc. 25th ICRC(Durban), **1**, 273.
- Jokipii, J. R, 1971, Rev. Geophys and Space Phys., **9**, 27.
- Jokipii, J. R, 1973, ApJ. **182**, 585.
- Kota, J.E., et.al., 1982, ApJ., **254**, 398.
- Ng, C.K., 1976, Proc. 17th ICRC(Paris), **3**, 389.
- Reid, G.C., 1964, JGR., **69**, 2659.
- Ruffolo, D, ApJ, 1995, **442**, 86.
- Volk, H., 1975, Rev. Geophys and Space Phys., **13**, 547.
- Zhang, D. L., 1993, Proc. 23rd ICRC(Calgary), **3**, 143.

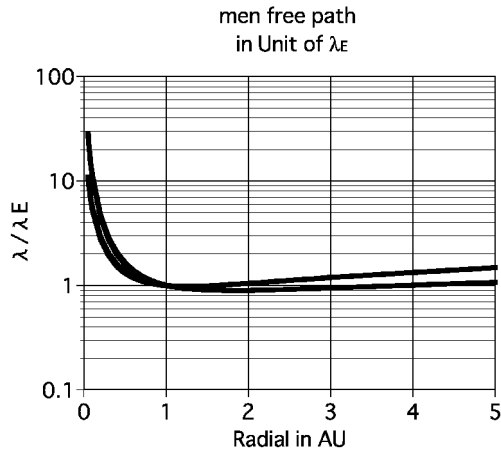


Figure 1

The upper curve beyond 1 AU shows $q=1.5$, the lower $q=1.67$.
The other parameters are $k=2$ and $m=0.5$.

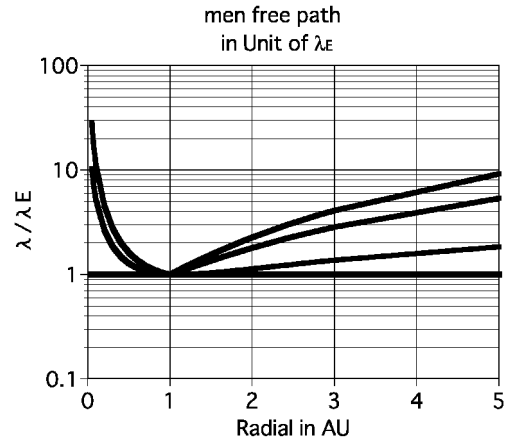


Figure 2

The uppermost curve corresponds to $k=2\sim3, m=0.5$, the
upper to $k=2\sim3, m=0$, the lower to $k=2, m=0.5$, the lowest to constant

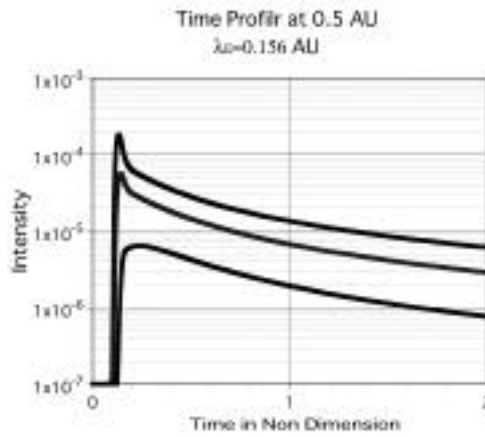


Figure 3

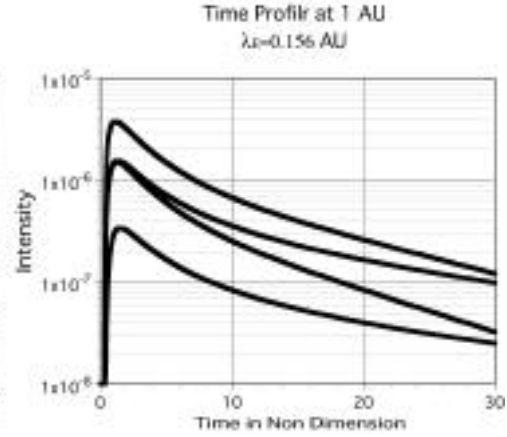


Figure 4

The uppermost curve corresponds to $k=2\sim3, m=0.5$, the upper to $k=2\sim3, m=0$, the lower to $k=2, m=0.5$, the lowest to constant

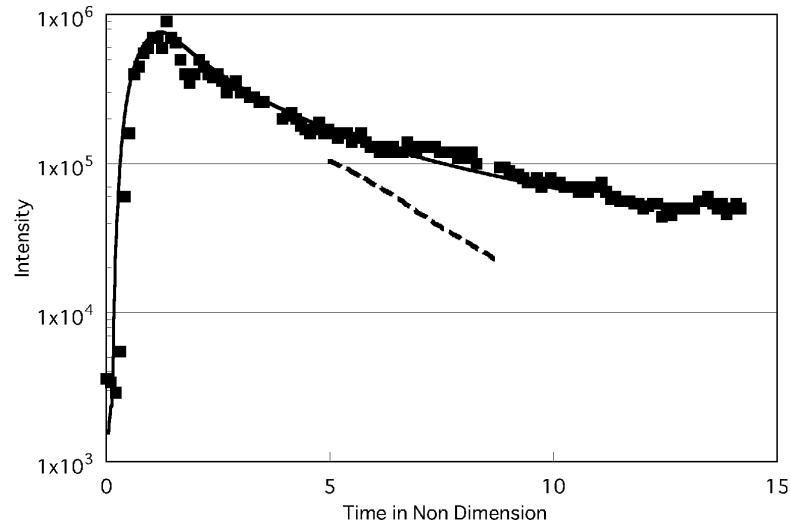


Figure 5

The solid squares denote observation on Helios 2, the solid line our case, and the dashed line taken from Bieber et al.,(1980)